










# NirA Is an Alternative Nitrite Reductase from *Pseudomonas aeruginosa* with Potential as an Antivirulence Target

 Samuel Fenn,<sup>a</sup>
 Jean-Frédéric Dubern,<sup>a</sup>
 Cristina Cigana,<sup>b</sup>
 Maura De Simone,<sup>b\*</sup> James Lazenby,<sup>a\*</sup> Mario Juhas,<sup>c\*</sup>
 Stephan Schwager,<sup>c</sup> Irene Bianconi,<sup>b\*</sup> Gerd Döring,<sup>†</sup> Jonas Elmsley,<sup>a</sup>
 Leo Eberl,<sup>c</sup>
 Paul Williams,<sup>a</sup>
 Alessandra Bragonzi,<sup>b</sup>
 Miguel Cámara<sup>a</sup>

<sup>a</sup>National Biofilms Innovation Centre, Nottingham University Biodiscovery Institute, School of Life Sciences, University of Nottingham, Nottingham, United Kingdom

<sup>b</sup>Division of Immunology, Transplantation and Infectious Diseases, IRCCS San Raffaele Scientific Institute, Milan, Italy

<sup>c</sup>Department of Microbiology, Institute of Plant Biology, University of Zürich, Zürich, Switzerland

<sup>d</sup>Institute of Medical Microbiology and Hygiene, University of Tübingen, Tübingen, Germany

**ABSTRACT** The opportunistic pathogen *Pseudomonas aeruginosa* produces an arsenal of virulence factors causing a wide range of diseases in multiple hosts and is difficult to eradicate due to its intrinsic resistance to antibiotics. With the antibacterial pipeline drying up, antivirulence therapy has become an attractive alternative strategy to the traditional use of antibiotics to treat *P. aeruginosa* infections. To identify *P. aeruginosa* genes required for virulence in multiple hosts, a random library of Tn5 mutants in strain PAO1-L was previously screened *in vitro* for those showing pleiotropic effects in the production of virulence phenotypes. Using this strategy, we identified a Tn5 mutant with an insertion in PA4130 showing reduced levels of a number of virulence traits *in vitro*. Construction of an isogenic mutant in this gene presented results similar to those for the Tn5 mutant. Furthermore, the PA4130 isogenic mutant showed substantial attenuation in disease models of *Drosophila melanogaster* and *Caenorhabditis elegans* as well as reduced toxicity in human cell lines. Mice infected with this mutant demonstrated an 80% increased survival rate in acute and agar bead lung infection models. PA4130 codes for a protein with homology to nitrite and sulfite reductases. Overexpression of PA4130 in the presence of the siroheme synthase CysG enabled its purification as a soluble protein. Methyl viologen oxidation assays with purified PA4130 showed that this enzyme is a nitrite reductase operating in a ferredoxin-dependent manner. The preference for nitrite and production of ammonium revealed that PA4130 is an ammonia:ferredoxin nitrite reductase and hence was named NirA.

**IMPORTANCE** The emergence of widespread antimicrobial resistance has led to the need for development of novel therapeutic interventions. Antivirulence strategies are an attractive alternative to classic antimicrobial therapy; however, they require identification of new specific targets which can be exploited in drug discovery programs. The host-specific nature of *P. aeruginosa* virulence adds complexity to the discovery of these types of targets. Using a sequence of *in vitro* assays and phylogenetically diverse *in vivo* disease models, we have identified a PA4130 mutant with reduced production in a number of virulence traits and severe attenuation across all infection models tested. Characterization of PA4130 revealed that it is a ferredoxin-nitrite reductase and hence was named NirA. These results, together with attenuation of *nirA* mutants in different clinical isolates, high level conservation of its gene product in *P. aeruginosa* genomes, and the lack of orthologues in human genomes, make NirA an attractive antivirulence target.

**KEYWORDS** *Pseudomonas aeruginosa*, virulence target, nitrite reductase, transposon mutagenesis, genome-wide screening, disease model, disease models, virulence determinants

**Citation** Fenn S, Dubern J-F, Cigana C, De Simone M, Lazenby J, Juhas M, Schwager S, Bianconi I, Döring G, Elmsley J, Eberl L, Williams P, Bragonzi A, Cámara M. 2021. NirA is an alternative nitrite reductase from *Pseudomonas aeruginosa* with potential as an antivirulence target. mBio 12:e00207-21. <https://doi.org/10.1128/mBio.00207-21>.

**Editor** Joanna B. Goldberg, Emory University School of Medicine

**Copyright** © 2021 Fenn et al. This is an open-access article distributed under the terms of the [Creative Commons Attribution 4.0 International license](https://creativecommons.org/licenses/by/4.0/).

Address correspondence to Samuel Fenn, [Samuel.fenn1@nottingham.ac.uk](mailto:Samuel.fenn1@nottingham.ac.uk), or Miguel Cámara, [Miguel.Camara@nottingham.ac.uk](mailto:Miguel.Camara@nottingham.ac.uk).

\* Present address: Maura De Simone, GLP Test Facility, San Raffaele Telethon Institute for Gene Therapy, IRCCS San Raffaele Scientific Institute, Milan, Italy; James Lazenby, Quadram Institute Bioscience, Norwich Research Park, Norwich, Norfolk, United Kingdom; Mario Juhas, Institute of Medical Microbiology, University of Zürich, Zürich, Switzerland; Irene Bianconi, Department of Cellular, Computational and Integrative Biology, CIBIO University of Trento, Trento, Italy.

† Gerd Döring passed away 2 July 2013.

**Received** 25 January 2021

**Accepted** 15 March 2021

**Published** 20 April 2021

**P***seudomonas aeruginosa* is a genetically versatile opportunistic pathogen, able to colonize and survive in multiple environments and hosts. This versatility underpins the ability of *P. aeruginosa* to cause a wide range of infections, commonly affecting the respiratory tract, burn wounds, urinary tract, bloodstream, cornea, skin, and soft tissue (1). The majority of these infections are nosocomial, with infections in immunocompromised hosts often life-threatening.

*P. aeruginosa* has gained notoriety as a member of the ESKAPE (*Enterococcus faecium*, *Staphylococcus aureus*, *Klebsiella pneumoniae*, *Acinetobacter baumannii*, *Pseudomonas aeruginosa*, and *Enterobacter* species) pathogens (2). These pathogens are differentiated according to their clinical relevance and capacity to become multi-drug resistant (MDR). Often treatment of *P. aeruginosa* is unsuccessful due to high levels of intrinsic and acquired antimicrobial resistance with biofilm formation promoting antimicrobial tolerance (3, 4).

Although carbapenem-resistant *P. aeruginosa* has been listed as “priority one” by the World Health Organization for the development of new antimicrobials, no new drugs with a novel mechanism of action against this organism have reached the market in recent years (5). Hence, there is a pressing need for the discovery of novel alternative strategies to the traditional use of antibiotics to treat *P. aeruginosa* infections. Antivirulence therapeutic approaches offer an attractive alternative strategy for developing drugs with high specificity and narrow spectra as they reduce the illness caused by the pathogen (“pathogen limitation”) instead of reducing pathogen burden directly (“pathogen elimination”) (6).

In recent years, vast progress has been made on the identification of *P. aeruginosa* virulence factors, unravelling the mechanisms they employ to cause disease and developing inhibitors which can inactivate them (7–12). While these studies have uncovered numerous promising small virulence inhibitor molecules, none has yet made it to the clinic. This has been influenced by many different factors, including the reliance on a single disease model, potential target conservation within the microbiota, a lack of understanding of target functionality, and the inability to define success when searching for inhibitors (13).

The sequencing of the first *P. aeruginosa* genome in 2000 revealed that the PAO1 strain sequenced (PAO1-UW) has a genome size of 6.3 Mbp and contains 5,570 open reading frames, making it the largest bacterial genome sequenced at the time (14). This large genome underpins the extensive metabolic and regulatory network providing *P. aeruginosa* with the genetic versatility to colonize multiple environments, hosts, and host sites. Besides, with the function of only 22.7% of *P. aeruginosa* genes experimentally demonstrated and close to 2,000 genes without functional annotation (15), there is still a large amount of information missing with regard to the mechanisms by which this organism causes disease, and potentially a vast array of novel *P. aeruginosa* virulence targets remains to be discovered.

Early studies suggested that virulence mechanisms employed by *P. aeruginosa* to infect phylogenetically diverse hosts are remarkably well conserved. Comparison of infection mechanisms in the plant *Arabidopsis thaliana* and mice revealed that *P. aeruginosa* uses a shared subset of virulence genes to provoke disease (16). The conserved nature of *P. aeruginosa* virulence suggested that use of a single disease model is sufficient to dissect *P. aeruginosa* virulence in all hosts (17), with various studies utilizing the nematode *Caenorhabditis elegans* (18), fruit fly *Drosophila melanogaster* (19), silkworm *Bombyx mori* (20), *Galleria mellonella* larvae (21), and zebrafish embryos (22). However, limitations of these studies are related to the impact of virulence in multihost system and the number of *P. aeruginosa* strains tested.

A study performed by our group combining whole-genome transposon mutagenesis with a cascade of *in vitro* and *in vivo* infection models uncovered the host-specific nature of *P. aeruginosa* virulence (23). This revealed a remarkably low overlap in virulence factor requirements between different models, suggesting that many of the virulence factors identified with single model studies may not represent virulence factors

required during human disease (23). Given the broad range of clinical manifestations exhibited by *P. aeruginosa* infections, it stands to reason that virulence genes identified as attenuated in multiple models are more likely to be both relevant to human disease and at multiple infection sites, representing promising antivirulence targets.

This study builds upon the successful whole-genome transposon mutant screening to identify novel *P. aeruginosa* virulence target genes (23). Here, we describe the identification of an additional mutant from this library on a yet uncharacterized gene of *P. aeruginosa*, PA4130, exhibiting attenuation in all infection models tested. Functional characterization revealed that PA4130 encodes an assimilatory nitrite reductase with a potential role in nitrogen source metabolism during *P. aeruginosa* pathogenesis. The attenuation in all disease models tested and the lack of human homologues make this nitrite reductase a promising antivirulence therapeutic target.

## RESULTS

**Isolation of an *P. aeruginosa* mutant attenuated in multiple virulence factor production.** To isolate novel virulence genes, a transposon (Tn5) insertion library was generated in a wild-type PAO1-L strain (23). A total of 57,360 individual colonies were picked and screened for pleiotropic attenuation in virulence phenotypes (reduced swarming and exoprotease and pyocyanin production) (23). Using the same screening approach, in the current study, a further transposon mutant (PAJD21) was isolated from the library. This mutant displayed reduced levels of pyocyanin and pyoverdine production as well as decreased swarming motility, with twitching, swimming, protease, and elastase activity being unaffected compared to that of the wild type (Fig. 1A to D; see also Table S1 in the supplemental material). Nucleotide sequence analysis of the Tn5-flanking region showed that the transposon had inserted into PA4130, encoding a hypothetical protein with homology to nitrite and sulfite reductases, and forming a predicted operon with PA4129 (Fig. 1E). To ensure the attenuation in virulence traits observed was not due a polar effect on PA4129, located in the same predicted transcriptional unit as PA4130, in-frame deletion mutants of both PA4130 and PA4129 were constructed to generate strains PAJD25 and PASF06, respectively. These isogenic mutants showed no growth differences in either lysogeny broth (LB) or artificial sputum medium (ASM) in relation to the parental strain (see Fig. S2 in the supplemental material).

The PAJD25 strain showed phenotypes similar to those of the Tn5 mutant PAJD21, with pyocyanin and pyoverdine reduced in both LB and ASM and swarming motility also impeded. Chromosomal complementation of PAJD25 with PA4130 restored pyocyanin and swarming motility to wild-type levels, with partial restoration of pyoverdine production (Fig. 1A to D). In contrast, the PA4129 deletion mutant PASF06 did not show any significant alterations in the virulence-related phenotypes (Table S3). This demonstrates that the phenotypes observed are specific to the mutation of PA4130.

When identifying new virulence targets, it is paramount to ensure they are conserved in a wide range of strains. To establish this, a nucleotide BLAST search of PA4130 against the NCBI *P. aeruginosa* taxonomic identifier database (taxid 287) revealed that this hypothetical protein is highly conserved, with 363/367 of the available genomes encoding a PA4130 orthologue. To determine whether PA4130 has a similar role in the virulence of *P. aeruginosa* strains from different sublines, in-frame PA4130 deletion mutants were created in the clinical isolates PA7 Bo599, PA14 AUS471, and LESB58 PA-W39. Deletion of PA4130 across all these strains resulted in a similar attenuation for both pyocyanin production and swarming motility, while protease production and growth remained unaffected, validating the results obtained for PAJD21 and PAJD25 (Fig. 2A to C and Table S4). In contrast, reduction in pyoverdine production was not conserved with no consistent pattern emerging between strains (Table S4). The similar phenotypes observed in the PA4130 deletion strains across phylogenetically diverse *P. aeruginosa* strains confirms PA4130 is not a PAO1-L specific virulence determinant. This supported the use of PAO1-L and the derived strain PAJD25 as representative strains to further characterize the role of PA4130 in virulence.

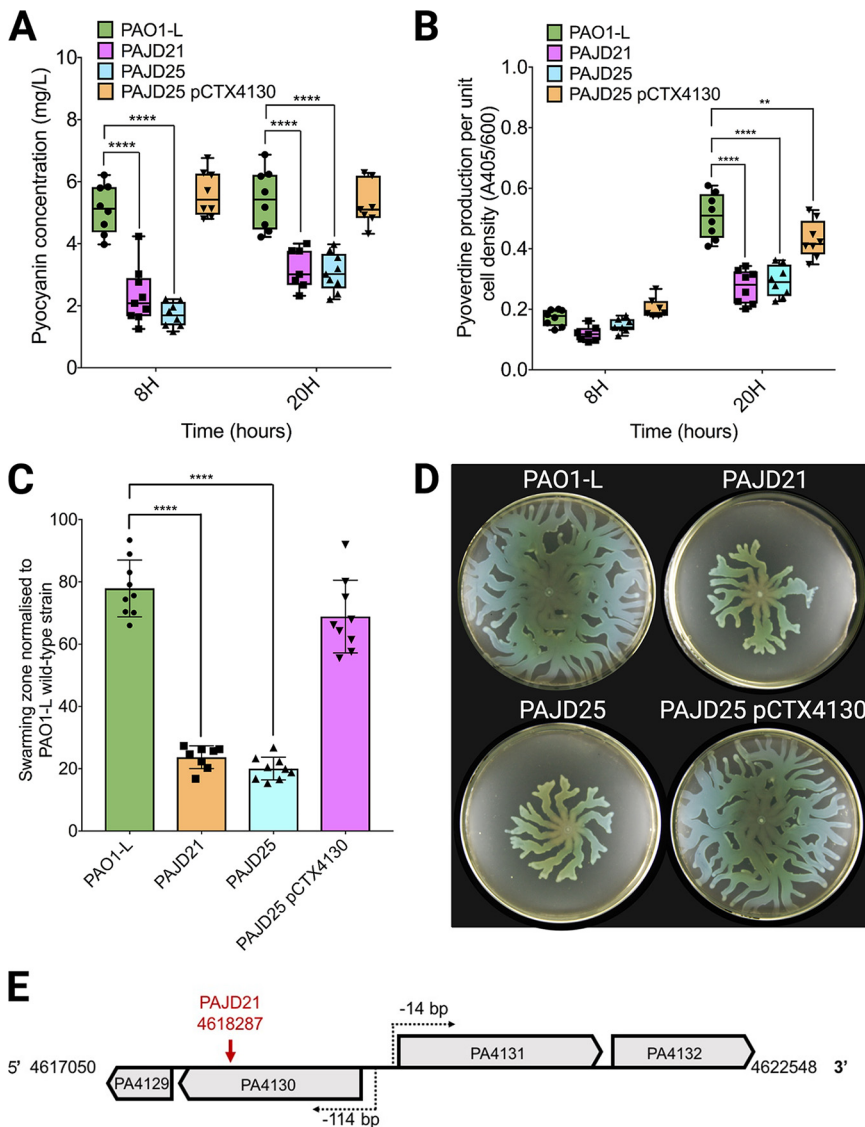


**FIG 1** *In vitro* phenotypic characterization of *P. aeruginosa* PAO1-L virulence factor production versus PA4130 mutants. The transposon mutant PAJD21 (PA4130::Tn5), the PA4130 in-frame deletion mutant PAJD25, and the complemented mutant PAJD25 pCTX4130 were used in these experiments. (A) Pyocyanin levels determined in supernatants from cultures grown for 8 and 20 h in LB using a colorimetric assay. (B) Pyoverdine levels determined in supernatants from cultures grown for 8 and 24 h in modified artificial sputum medium using a colorimetric assay. A405/600, absorbance at 405 and 600 nm. (C and D) Swarming motility surface coverage measurements (C) and images (D); cells were inoculated from a 16-h LB culture onto swarming plates containing 0.5% agar and incubated at 37°C for 16 h. (E) Diagram displaying operon structure and transcriptional start sites of PA4129-PA4130 and PA4131-PA4132 with the PAJD21 Tn5 insertion site indicated by the red arrow. Data were collated from three independent experiments with at least three replicates each. Values that are significantly different by Dunnett’s multiple-comparison test are indicated by asterisks as follows: \*\*,  $P < 0.01$ ; \*\*\*\*,  $P < 0.0001$ .

**PA4130 is required for full virulence in *C. elegans* and *D. melanogaster*.** To establish whether the decrease in virulence trait production observed in the PA4130 deletion mutant PAJD25 *in vitro* also results in disease attenuation *in vivo*, the *D. melanogaster* and *C. elegans* nonmammalian infection models previously used for *P. aeruginosa* infection studies were initially used. In both disease models, the PAJD25 ( $\Delta$ PA4130) mutant showed an attenuated survival rate compared to that of the isogenic wild-type PAO1-L (Fig. 3). For *C. elegans*, PAJD25 virulence was severely attenuated with a 57% increase in survival at 72 h postinfection (Fig. 3A). In the case of *D.*

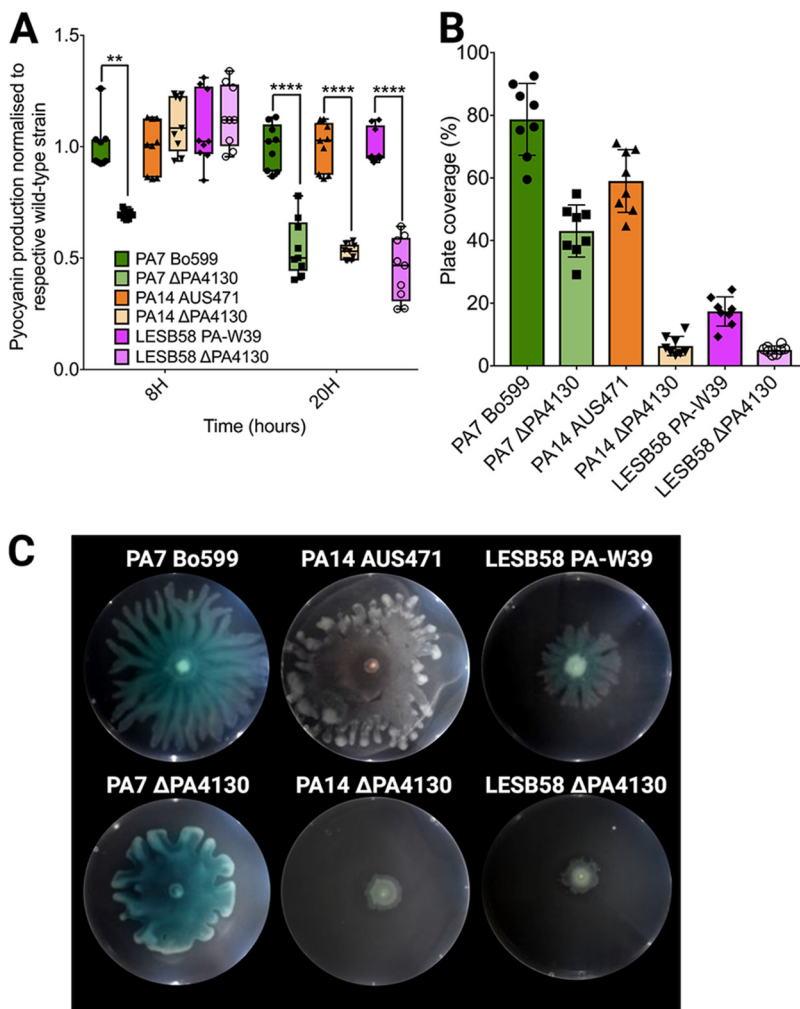


**FIG 2** *In vitro* phenotypic characterization of virulence factor production for PA4130 orthologue mutants in PA7 Bo599, PA14 AUS471, and LESB58 PA-W39. (A) Pyocyanin levels determined in supernatants from cultures grown for 8 and 20 h in LB using a colorimetric assay. (B and C) Swarming motility surface coverage measurements (B) and images (C); cells were inoculated from a 16-h LB culture onto swarming plates containing 0.5% agar and incubated at 37°C for 20 h. Data were collated from two independent experiments with at least four replicates. Values that are significantly different by Tukey's multiple-comparison test are indicated by asterisks as follows: \*,  $P < 0.05$ , \*\*,  $P < 0.01$ , \*\*\*\*,  $P < 0.0001$ .

*melanogaster*, PAJD25 killing was delayed with a 40% increase in survival at 18 h post-infection, although by 22 h, this difference was negligible (Fig. 3A).

**Deletion of PA4130 results in reduced cytotoxicity, cellular invasion, and IL-8 production in A549 human lung epithelial cell line.** A previous screening of the Tn5 mutant library screening by Dubern and colleagues (23) suggested that attenuation using *in vitro* assays and invertebrate infection models does not translate into mammalian models. To establish whether this is the case for the PA4130 mutant, the PAJD25 ( $\Delta$ PA4130) strain was tested on the A549 pulmonary cell line for cytotoxicity, invasion, and interleukin 8 (IL-8) production (Fig. 4). Cytotoxicity of the PAJD25 supernatant was drastically reduced compared to strain PAO1-L, which is in line with the reduced levels of secreted pyocyanin (Fig. 1A and 4A). Furthermore, invasion of A549 epithelial cells was reduced in strain PAJD25, with IL-8 production also reduced compared to wild-type strain PAO1-L (Fig. 4B and C).

**Deletion of PA4130 reduces lethality of *P. aeruginosa* in acute and agar bead murine infection models.** The impact of a PA4130 mutation on *P. aeruginosa* virulence was initially assessed by determining the survival curve of PJD25 ( $\Delta$ PA4130) in an acute



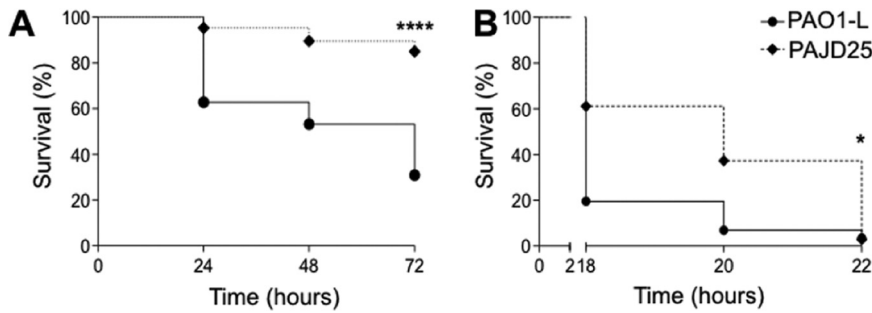


**FIG 3** Survival of strain PAO1-L versus strain PAJD25 in nonmammalian models. (A) 72-h lethality curve in the *C. elegans* infection model. (B) 22-h lethality curve in *D. melanogaster*. Both models demonstrated clear attenuation with increased survival of PAJD25 in *C. elegans* at all time points. *D. melanogaster* exhibited a delay in killing with increased survival at earlier time points; however, by 22 h, both PAO1-L and PAJD25 showed almost complete killing. The results presented display the mean values from three independent experiments. \*,  $P < 0.032$ , \*\*\*\*,  $P < 0.0001$  log rank Mantel-Cox test.

lung infection model in C57BL/6NCrIBR mice using an infection dose of  $5 \times 10^6$  CFU. A survival rate of 80% was shown at 72 h postinfection in contrast to strain PAO1-L which did not show any survival after 36 h (Fig. 5).

The effect of the PA4130 mutation was then tested in an agar bead infection model to monitor initial colonization and systemic spread. C57BL/6NCrIBR mice were infected with a  $2 \times 10^6$  CFU dose of either strain PAO1-L or PAJD25. At 18 h postinfection, 20% of PAO1-L-infected mice and 80% of PAJD25-infected mice survive. By 36 h, 80% of PAJD25-challenged mice still survive while PAO1-L-infected mice exhibit no survival (Fig. 6A). The reduction in mortality was confirmed by the reduced CFU recovery from the lung, liver, and spleen of the mutant compared to the wild type (Fig. 6B to D). Clearance or reduced CFU in the lung of PAJD25-infected mice demonstrates that interruption of PA4130 interferes with colonization. This impaired colonization results in reduced systemic spread with no PAJD25 detected in the spleen or liver in all but one sample (Fig. 6B to D).

Overall, the data presented demonstrate that PA4130 plays a role in *P. aeruginosa* survival and virulence in multiple models of infection, suggesting that PA4130 is not a model-specific virulence gene.

**Purification of PA4130 reveals characteristics of a possible nitrite or sulfite reductase.** Amino acid sequence analysis showed that PA4130 has an amino acid similarity of 21% with the *Escherichia coli* CysI sulfite reductase hemoprotein subunit and that no protein homologues are encoded within the human genome. Alignment of the

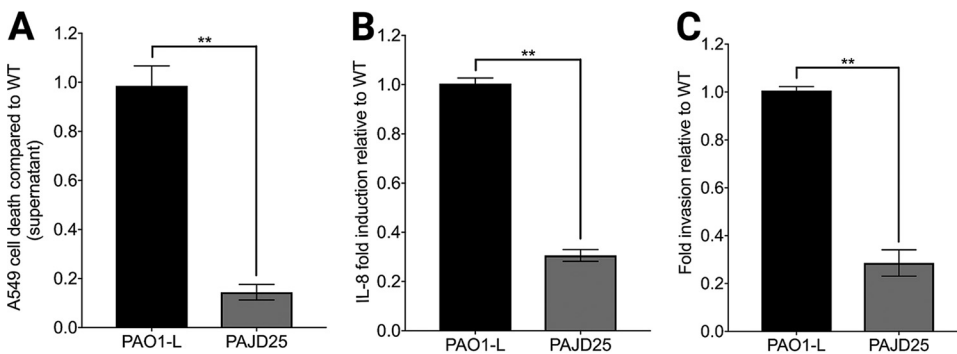


**FIG 4** Cytotoxicity, IL-8 release, and invasion of A549 cells following infection with either strain PAO1-L or PAJD25. (A) Cytotoxicity assayed with Syto13/propidium iodine (PI) viability staining. WT, wild type. (B) IL-8 released quantified by enzyme-linked immunosorbent assay (ELISA) following infection. (C) Invasion quantified using an antibiotic (polymyxin B) exclusion assay. Data from three independent experiments are expressed as means  $\pm$  standard errors of means (SEM) (error bars). \*\*,  $P < 0.01$  by Student's *t* test.

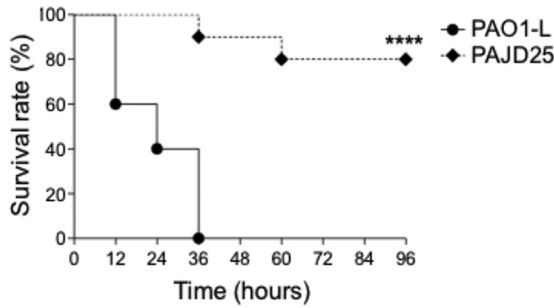


**FIG 5** Survival curve of C57BL/6NCrIBR mice infected with strains PAO1-L and PAJD25 in an acute lung infection model. At 36 h, PAJD25 exhibits a 90% increase in survival compared to PAO1-L, with 80% of PAJD25-infected mice surviving past 96 h. \*\*\*\*,  $P < 0.0001$  by log rank Mantel-Cox test.

PA4130 amino acid sequence with the *E. coli* MG1655 CysI, *Mycobacterium tuberculosis* H37RV NirA, and *Spinacea oleracea* (spinach) NirA, using ClustalW, revealed the presence of conserved residues indicative of 4Fe-4S and siroheme prosthetic group binding sites (Fig. S2). Initial expression and purification attempts yielded insoluble, non-functional PA4130. Prosthetic group limitation was hypothesized to limit soluble PA4130 expression. Coexpression of iron-sulfur cluster biogenesis or siroheme synthesis proteins has been demonstrated to increase expression of functional enzymes incorporating these prosthetic groups (24, 25). PA4130 was subsequently coexpressed in the presence of the siroheme synthase CysG, yielding a 20-fold increase in soluble PA4130 expression. PA4130 was purified to homogeneity with a combination of immobilized metal affinity chromatography and chitin column chromatography, while size exclusion chromatography revealed PA4130 is a monomer in solution

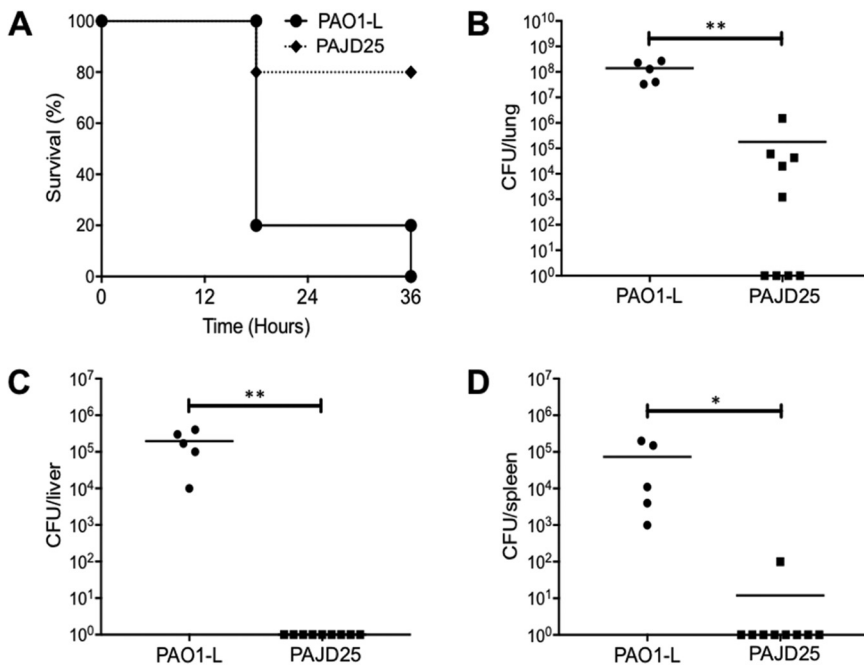


**FIG 6** Virulence of strains PAO1-L and PAJD25 in an agar bead murine lung infection model of colonization in C57BL/6NCrIBR mice. (A to D) Survival curve (A), CFU recovery from lung (B), CFU recovery from the liver (C) and CFU recovery from the spleen at 36 h postinfection (D). Strain PAJD25 exhibits a significant increase in survival at 36 h postinoculation with a CFU recovery 3 log units lower than that of strain PAO1-L in the lungs. PAO1-L infection progresses to the liver and spleen within 36 h, while PAJD25 infection does not proceed to the liver and spleen as indicated by the absence of CFU recovery in all but one sample. \*\*\*\*,  $P < 0.0001$  by log rank Mantel-Cox test for survival curve. \*,  $P < 0.05$ ; \*\*,  $P < 0.01$  by Student's *t* test for CFU recovery.

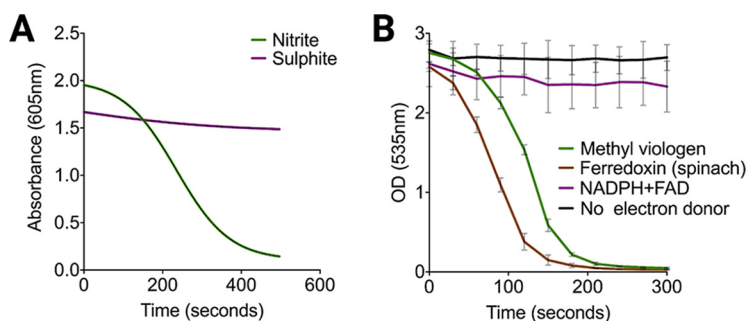


**FIG 7** PA4130-mediated reduction assays for native electron acceptor and donor determination. (A) Methyl viologen oxidation assay in the presence of the electron acceptors nitrite and sulfite. Reduced MV is oxidized only in the presence of nitrite, indicating PA4130 is a nitrite reductase. (B) Nitrite reduction assay using MV, reduced ferredoxin, and NADPH as electron donors. The remaining nitrite was quantified by Griess diazotization, with nitrite reduction occurring in the presence of MV and reduced ferredoxin.

(Fig. S3). Spectroscopic characterization of the soluble PA4130 protein confirmed the presence of peaks at 382 nm, 587 nm, and 712 nm, characteristic of siroheme and 4Fe-4S incorporation into nitrite/sulfite reductase hemoprotein subunits (data not shown).

**PA4130 codes for an assimilatory nitrite reductase operating in a ferredoxin-dependent manner.** Nitrite or sulfite reductases catalyze the six-electron reduction of nitrite or sulfite to ammonium or hydrogen sulfide, respectively. These enzymes require an electron acceptor and donor to complete the electron transport chain. The electron acceptor is nitrite or sulfite with the electron donor being either NADPH, NADH, or ferredoxin.

To determine the native electron acceptor, we used a reduced methyl viologen (MV) reductase assay, which spectrophotometrically tracks the artificial electron donor oxidation in the presence of nitrite or sulfite as the possible electron acceptor for PA4130 (26). Our data show that PA4130 was able to oxidize MV only in the presence of nitrite with minimal oxidation occurring in the presence of sulfite (Fig. 7A). These results confirm that PA4130 functions as a nitrite reductase and hence participates in the nitrate reduction pathway.

To identify the native electron donor used by PA4130, the same assay as described above was carried out with the alternative electron donors NADPH+FAD and reduced spinach ferredoxin, with the remaining nitrite quantified using Griess diazotization. Tracking of the remaining nitrite revealed that reduction occurs only in the presence of MV and reduced ferredoxin while minimal reduction occurs with NADPH plus FAD (Fig. 7B). This observation is in agreement with a study by Frangipani and colleagues showing that increased expression of both PA4130 and the ferredoxin:NADP<sup>+</sup> reductase *fprA* are induced by cyanogenesis in *P. aeruginosa* (27). This suggests that the role of FprA is to reduce ferredoxins, using NADPH as an electron donor, ensuring a supply of reduced ferredoxin for PA4130 to derive electrons for nitrite reduction.

The nitrite reductase cognate pathways can be assigned via the end reaction product. Nitric oxide (NO)-forming nitrite reductases participate in the dissimilatory denitrification pathway, while ammonium (NH<sub>4</sub><sup>+</sup>)-producing reductases are part of either assimilatory or dissimilatory nitrite reduction to ammonium (DNRA) pathways (Fig. 8) (28). *P. aeruginosa* genes encode three structurally distinct nitrite reductases, the NO-forming denitrification reductase NirS, NH<sub>4</sub><sup>+</sup>-forming NirBD, and unassigned PA4130. Conserved domain analysis using DELTA-BLAST suggests that PA4130 resembles an ammonium-producing nitrite reductase. This was confirmed with an ammonium production assay following nitrite reduction using reduced ferredoxin as an artificial electron donor (Fig. S4).

Together, these data indicate that PA4130 codes for an ammonium-producing, ferredoxin- and siroheme-dependent, nitrite reductase, which participates in the nitrate



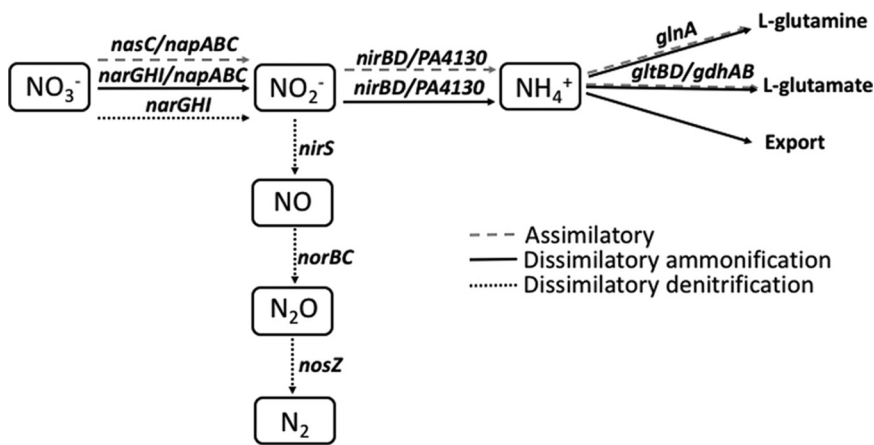


**FIG 8** Genetic and biochemical pathways involved in nitrate reduction. This highly branched process is divided into three primary pathways: assimilatory and dissimilatory nitrite reduction to ammonium (DNRA) and dissimilatory denitrification. The presence of multiple pathways enables multiple biological functions to be performed with amino acid synthesis, detoxification, energy generation, and conservation key to survival in diverse environments.

reduction cycle. We propose that PA4130 be renamed NirA to fit with current nomenclature.

## DISCUSSION

In a previous study, we aimed to identify novel genes required for virulence in *P. aeruginosa* using a multihost screening strategy with the ultimate goal of discovering novel antivirulence targets (23). Using the same strategy we have identified, a new Tn5 mutation in PA4130 which is attenuated in multiple virulence factor production. One limitation previously identified with this screening strategy (23) was the use of a single strain of *P. aeruginosa*, as there can be significant variations between the virulence of different strains, potentially leading to the identification of strain-specific virulence factors (29). This problem was circumvented by generating PA4130 orthologue deletion mutants in phylogenetically distinct *P. aeruginosa* strains covering the major phylogenetic groups identified by Freschi and colleagues (30). This revealed a conserved role of PA4130 in virulence factor production with pyocyanin production and swarming motility being impaired across all mutants. Further screening revealed attenuation of a PA4130 mutant across all disease models tested in this study, confirming that PA4130 is not a disease model-specific virulence determinant and is likely to play a key role in survival during human infection. This makes PA4130 a promising target which can be taken forward for functional and structural characterization with a view to develop novel virulence inhibitors against this opportunistic pathogen.

Characterization of the predicted gene product of PA4130 showed an assimilatory ferredoxin-dependent nitrite reductase likely involved in nitrate and wider central nitrogen metabolism. Hence, it has subsequently been named *nirA*. Previous studies have also detected various carbon and nitrogen metabolic genes as essential for full virulence, since infection is associated with significant metabolic changes (23, 31, 32). Inhibiting adaptation to carbon and nitrogen sources or attenuating the ability to protect from nitrative stress during infection could prove an attractive antivirulence strategy with metabolic dysregulation having knockdown effects on multiple cellular cycles.

Nitrogen source metabolism is essential for the survival of *P. aeruginosa* in diverse environments enabling amino acid synthesis, carbon source utilization, and respiration in the absence of oxygen (31). A key element to nitrogen source metabolism is the reduction of nitrate. *P. aeruginosa* nitrate metabolism is a highly branched and

interlinked process with three main pathways, dissimilatory denitrification, dissimilatory nitrate reduction to ammonium (DNRA), and assimilatory nitrate reduction to ammonium (Fig. 8) (28, 33).

Dissimilatory denitrification in *P. aeruginosa* reduces nitrate to gaseous dinitrogen, coupling reduction to generation of a proton gradient. This facilitates respiration in the absence of oxygen. The assimilatory pathway is dedicated to biosynthesis, with the assimilatory nitrate reductase (NasC) and assimilatory nitrite reductase (NirBD) producing nitrogen in the form of ammonium. DNRA differs, requiring the respiratory nitrate reductases NarGHI or NapABC to enable energy generation/conservation (28, 33) while simultaneously maintaining intracellular level of nitrogen via the production of ammonium.

The NirA production of ammonium *in vitro* suggests that it participates in either assimilatory or DNRA with potential implications in amino acid biosynthesis, energy conservation, detoxification, and maintenance of the intracellular redox environment (28, 34). However, determining the exact role NirA plays during virulence is complicated by the fact that *P. aeruginosa* genes code for two additional producing nitrite reductases, nitric oxide-forming NirS and ammonium-forming NirBD.

NirS is a component of the dissimilatory denitrification pathway and reduces nitrite to nitric oxide (NO). Various components of the dissimilatory nitrate reduction pathway have been demonstrated to be attenuated for virulence, with deletion of NirS in PA14 reported to be avirulent in *C. elegans* and the THP-1 human monocyte cell line (35, 36). However, these NirS-dependent phenotypes have been attributed to production of NO which modulates type III secretion system expression (36). Since NirA is an NH<sub>4</sub>-forming nitrite reductase, it participates in a separate part of the nitrate reductase pathway (Fig. 8), with the resulting phenotypes independent of NO production.

Although NirBD and NirA perform the same molecular function, they are differentially regulated. *nirBD-PA1779(nasC)-cobA* are under the control of the RpoN nitrogen utilization sigma factor, with NtrC and NasT acting as transcriptional activators. Expression occurs under low nitrogen availability in the presence of nitrate and nitrite (37). In contrast, NirA expression is under the control of cyanogenesis and is involved in protecting cells from HCN self-intoxication alongside PA4129-34 and *cioAB* by a yet undefined mechanism (27).

The role played by these ammonium-forming nitrite reductases during pathogenesis has largely remained unexplored *in vivo* with the exception of *M. tuberculosis*, where induction of *nirBD* is required for survival in human macrophages during hypoxia (38). Animals and plants produce reactive nitrogen species (RNS) in response to diverse bacterial infections (39). Host-derived RNS originate from inducible and constitutively expressed nitric oxide synthases (iNOS), with subsequent autooxidation resulting in formation of nitrate and nitrite (40). *P. aeruginosa* is capable of detoxifying these RNS and actively uses them for respiration and macromolecule biosynthesis, thriving under challenging conditions.

With induction of *nirA* under the control of HCN, maximal expression will occur under microaerobic conditions due to the dual action of Anr and the *las/rhl* quorum-sensing cascade (41). This suggests that NirA plays a similar role to NirBD of *M. tuberculosis*, allowing persistence or growth *in vivo* by protecting *P. aeruginosa* from nitrative stress under oxygen limiting conditions. Work is now ongoing to understand the role of NirA in virulence and how this overlaps with the function of NirBD, NirS, and cyanogenesis.

While the mechanisms are yet to be unraveled, the discovery that the nitrite reductase NirA is required for virulence in multiple infection models represents a very attractive prospect for the development of inhibitors. Humans do not reduce nitrate and nitrite and as such do not encode nitrite reductases, minimizing off-site effects of any inhibitors developed. Taking these points together makes NirA a promising antivirulence target candidate against *P. aeruginosa* infections.

## MATERIALS AND METHODS

**Bacterial strains, plasmids, growth conditions, and DNA manipulation.** Bacterial strains and plasmids are listed in Table S1 in the supplemental material. *P. aeruginosa* and *E. coli* were routinely cultured in lysogeny broth (LB) at 37°C with vigorous shaking (200 rpm), unless otherwise stated. Artificial sputum medium (ASM) was made according to reference 42, modified with the addition of 0.5 mM KNO<sub>3</sub> to replicate conditions reported in the cystic fibrosis (CF) lung (43, 44). Media were solidified with 1.5% agar. Antibiotics were added, when required, at concentrations of 20 µg ml<sup>-1</sup> for gentamicin, 15 µg ml<sup>-1</sup> for nalidixic acid, and 20 µg ml<sup>-1</sup> for streptomycin. Tetracycline was added at a final concentration of 150 µg ml<sup>-1</sup> for *P. aeruginosa* and 10 µg ml<sup>-1</sup> for *E. coli*. Protein overexpression was performed in terrific broth (TB) (24 g/liter yeast extract, 12 g/liter tryptone, 4% glycerol, 0.017 M KH<sub>2</sub>PO<sub>4</sub>, and 0.072 K<sub>2</sub>HPO<sub>4</sub>) supplemented with 1 mM FeSO<sub>4</sub>·6H<sub>2</sub>O and 50 µg ml<sup>-1</sup> of carbenicillin and streptomycin.

Genomic DNA isolation was performed using a Wizard Genomic DNA purification kit (Promega). Plasmid isolation was performed with GenElute plasmid miniprep kit (Sigma). All other standard DNA manipulation techniques such as analysis, digestion, ligation, and transformation were performed according to Sambrook and Russell (45).

**Mutant selection and phenotype confirmation.** A previously reported *P. aeruginosa* Tn5 mutant library was further screened for new mutants showing alterations in pyocyanin production, swarming motility, and alkaline protease activity with the aid of Flexis (Genomics solutions) colony-picking robot as previously described (23). Quantitative assays confirming observed phenotypes for pyocyanin, pyoverdine, swarming, and protease were evaluated as described elsewhere (46).

***C. elegans* and *D. melanogaster* virulence assays.** Both nematode slow killing assays and *D. melanogaster* disease models were performed as previously described (23, 47).

**Cell culture, IL-8 secretion, invasion, and cytotoxicity assays.** A549 (human type II pneumocytes) were purchased from ATCC and cultured as described previously (48). IL-8 secretion was performed as reported previously (23). Bacterial invasion was determined using a polymyxin B protection assay (23). Cytotoxicity of *P. aeruginosa* culture supernatant and cell pellet was assessed using the Syto-13/propidium iodide viability test according to reference 49.

**In-frame deletion mutant construction and complementation.** To construct an in-frame deletion in PA4130, two DNA fragments 427 bp upstream and 433 bp downstream from PA4130 were generated and fused by overlap extension PCR using PAO1-L genomic DNA as a template. The upstream 427-bp fragment was amplified with primers PA4130F1 which carries an XbaI restriction site and PA4130R1 containing the first 12 nucleotides of PA4130 with an overhanging end containing the last 15 nucleotides of the PA4130 ORF (Table S1); the downstream 433-bp fragment was amplified with PA4130F2 containing the last 15 nucleotides of PA4130 with an overhanging end containing the first 12 nucleotides and PA4130R2 containing a HindIII restriction site (Table S1). To perform the overlap extension PCR, a secondary PCR was performed with the 427-bp and 433-bp fragments serving as the templates and primers PA4130F1/PA4130R2 (Table S2). The final PCR product was cloned using the XbaI/HindIII restriction sites into the vector pME3087, resulting in the suicide plasmid pME4130. The suicide plasmid used to generate the PA4129 mutant was constructed as described above, using primer pairs PA4129F1/PA4129R1 and PA4129F2/PA4129R2 to generate two PCR products upstream and downstream of PA4129 and using primer pairs PA4129F1/PA4129R2 to generate the final PCR product containing a deletion in PA4129, which was cloned into pME3087, resulting in the suicide plasmid pME4129 (Table S2).

The PA4129 and PA4130 in-frame deletions were generated by allelic exchange using pME4129 and pME4130, respectively. Briefly, pME4129 and pME4130 were mobilized by conjugation into the relevant *P. aeruginosa* strains using *E. coli* S17.1 *λpir*. Conjugants were selected for on LB agar supplemented with tetracycline and nalidixic acid. Strains were restreaked twice on LB, with no antibiotic, and subjected to tetracycline sensitivity enrichment to select for double crossover events (49). Colonies were screened for loss of resistance to tetracycline with allelic exchange confirmed with PCR and DNA sequencing, resulting in strains PASF06 (ΔPA4129), PAJD25 (PAO1-L ΔPA4130), PA7 Bo599 ΔPA4130, PA14 AUS471 ΔPA4130, and LESB58 ΔPA4130 (Table S2).

Strain PAJD25 was complemented by amplifying a 2,172-bp fragment containing the PA4130 open reading frame (ORF) and +498 bp of the translational start site using primers 4130CTXF1/4130CTXR1. The PCR product was cloned into the integrative vector mini-CTX-1 using the HindIII/BamHI restriction sites, forming pCTX4130, with the resulting vector mobilized by conjugation, as performed with pME4129 and pME4130. Conjugants were selected on LB agar supplemented with tetracycline and nalidixic acid. The integration of pCTX4130 was confirmed using PCR and DNA sequencing with complementation demonstrated through restoration of pyocyanin production and swarming motility.

**Acute murine infection model.** C57BL/6NCR1BR male mice (8 to 10 weeks of age) were purchased from Charles River Laboratories, Italy. In the acute murine lung infection model, *P. aeruginosa* strains were grown for 3 h in tryptic soy broth (TSB). Bacteria were then harvested, washed twice with sterile phosphate-buffered saline (PBS), and resuspended in sterile PBS to the desired dose for infection of 5 × 10<sup>6</sup> CFU/mouse. Mice were anaesthetized, and the trachea were directly visualized by a ventral midline incision, exposed, and intubated with a sterile, flexible 22-g cannula attached to a 1-ml syringe accordingly to established procedures (48). A 60-µl inoculum of 5 × 10<sup>6</sup> CFU was implanted into the lung via cannula. Following infection, mice were monitored twice a day for 4 days. Mice that lost >20% body weight and presented signs of severe clinical disease were sacrificed by CO<sub>2</sub> administration before termination of the experiment. Further details are outlined in supplemental material.

**Agar bead infection model.** C57BL/6 male mice (6 to 10 weeks of age) were purchased from Charles River Laboratories, Germany. The agar bead mouse model was performed according to established procedures (50). Fresh cultures were prepared in 5 ml TSB and incubated for 3 h. Bacterial cells

were harvested and embedded in agar beads according to Bragonzi and colleagues (51). Five to 10 mice were used for experiments and intratracheally infected with  $4.6 \times 10^6$  CFU. Following infection, mice were monitored twice a day for 2 days. Mice that lost >20% body weight and presented signs of severe clinical disease were sacrificed by injection of 2 ml of 20% pentobarbital. For quantitative bacteriology, lung, liver, and spleen were excised aseptically and homogenized using the homogenizer DIAx 900 (Heidolph GmbH, Schwabach, Germany). Bacterial numbers in the organs were determined by 10-fold serial dilutions of the homogenates, spotted onto blood plates after incubation at 37°C for 18 h.

**Ethics statement.** Acute murine infection studies were conducted according to protocols approved by the San Raffaele Scientific Institute (Milan, Italy) Institutional Animal Care and Use Committee (IACUC) and adhered strictly to the Italian Ministry of Health guidelines for the use and care of experimental animals. Agar bead infection studies were conducted according to protocols approved by Institute of Medical Microbiology and Hygiene (Tübingen, Germany) and adhered strictly to guidelines set by the German Ministry of Health and Animal Welfare Institute (Baden-Württemberg).

**PA4130 expression and purification.** The PA4130 *orf* was amplified from PAO1 genomic DNA using primer pair NT4130F1/NT4130R1 containing N-terminal hexahistidyl tag and EcoRI/SacI restriction sites (Table S2). The modified PA4130 fragment was cloned into vector pSK67 using EcoRI/SacI restriction sites, resulting in plasmid pSK4130-N. The *cysG* *orf* was PCR amplified from *E. coli* BL21 (DE3) using primer pair CDFcysGF1/CDFcysGR1 containing restriction sites BglII/XhoI (Table S2). The modified *cysG* gene was inserted into vector pCDF-DUET1 using restriction sites BglII/XhoI, producing vector pCDF-cysG. The resulting pSK4130-N and pCDF-cysG coding sequences were confirmed with commercial Sanger sequencing.

Vectors pSK4130-N and pCDF-cysG were cotransformed into *E. coli* NiCo21 by electroporation with simultaneous selection of both vectors on LB agar plates using carbenicillin and streptomycin. Single colonies were selected and grown in LB broth for 16 h at 37°C. Cell density was then adjusted to an optical density (OD) of 0.05 into TB and further grown to an OD of ~0.6 to 0.8 (600 nm). Cultures were then cooled to 20°C before addition of 0.05 M ferric citrate and induction with 0.1 mM isopropyl- $\beta$ -D-thiogalactopyranoside. Following a further 18-h growth, cell pellets were harvested via centrifugation, flash frozen in liquid N<sub>2</sub>, and stored at -80°C.

For purification, a combination of immobilized metal ion affinity chromatography (IMAC), chitin column chromatography (CCC) used to obtain soluble PA4130. Frozen pellets were resuspended in lysis buffer consisting of 50 mM Tris-HCl, 150 mM NaCl, 1.2  $\mu$ g/ml lysozyme, and cOmplete Ultra EDTA-free protease inhibitor cocktail at pH 8.0 with 1 g cell paste per 10 ml of buffer. Samples were incubated on ice for ~30 min with membrane disruption achieved by sonication (Fisher model 505/705).

IMAC was performed with the HiTrap chelating HP column (GE Healthcare) charged with NiSO<sub>4</sub>. The column was equilibrated with 10 column volumes (CV) of buffer A containing 50 mM Tris-HCl, 500 mM NaCl, 5% glycerol, 20 mM imidazole at pH 8.0 before sample application with a peristaltic pump (GE Healthcare model P1). PA4130 was obtained using a linear imidazole gradient from 20 to 400 mM imidazole between buffer A and buffer B (buffer A with 400 mM imidazole) with red/brown samples collected and pooled together.

Following IMAC, samples were processed and applied to chitin resin according to the manufacturer's instructions (New England Biolabs). The CCC flowthrough harboring PA4130 was collected and analyzed by sodium dodecyl sulfate-polyacrylamide gel electrophoresis (SDS-PAGE) for homogeneity. For size-exclusion chromatography, samples were concentrated to 5 ml using a Vivaspinn centrifugal filter unit (Cytiva) and injected onto a 16/600 Superdex 200-pg column (Cytiva) and eluted with 50 mM Tris and 150 mM NaCl (pH 7.5).

**Reduced methyl viologen assay.** The PA4130 protein was tested for nitrite/sulfite reductase activity using the artificial electron donor methyl viologen (MV); the MV reduction reaction in the presence of sodium dithionite produces a blue coloration. The assay was adapted from an assay of Schnell and colleagues (25) under anaerobic conditions to prevent oxygen-dependent oxidation of MV. MV oxidation was tracked spectrophotometrically at 5-s intervals with nitrite, hydroxylamine, or sulfite acting as an electron acceptor.

**Griess diazotization and ammonia detection assays.** Griess diazotization was performed using the Griess reagent system (Promega) according to manufacturer's instructions. The assays were performed as described above, with the exception that the electron donors were altered. MV, spinach ferredoxin, and NADPH plus flavin mononucleotide (FMN) were used, with MV and ferredoxin artificially reduced using sodium dithionite. Temporal tracking of reduction reaction was achieved via sacrifice of eight independent reactions every 30 s.

Production of ammonia was confirmed using an ammonia assay kit (Sigma) according to the manufacturer's instructions.

## SUPPLEMENTAL MATERIAL

Supplemental material is available online only.

**FIG S1**, PDF file, 0.1 MB.

**FIG S2**, PDF file, 0.1 MB.

**FIG S3**, PDF file, 0.1 MB.

**FIG S4**, PDF file, 0.01 MB.

**TABLE S1**, DOCX file, 0.1 MB.

**TABLE S2**, DOCX file, 0.1 MB.

**TABLE S3**, DOCX file, 0.04 MB.

**TABLE S4**, DOCX file, 0.05 MB.

## ACKNOWLEDGMENTS

This study was supported by European Commission (grant NABATIVI, EU-FP7-HEALTH-2007-B, contract number 223670), Wellcome Trust AAMR DTP program (grant 108876/Z/15/Z), and Ministero della Salute (project GR/2009/1579812). M.C. and P.W. are partly funded by the National Biofilms Innovation Centre (NBIC) which is an Innovation and Knowledge Centre funded by the Biotechnology and Biological Sciences Research Council, InnovateUK, and Hartree Centre (award number BB/R012415/1).

We especially thank Annika Schmidt for her help in obtaining data from the lab of the late Gerd Döring. Her efforts have been invaluable in ensuring that the work of his lab and its previous members continues to gain the recognition it deserves.

## REFERENCES

- Gellatly SL, Hancock RE. 2013. *Pseudomonas aeruginosa*: new insights into pathogenesis and host defenses. *Pathog Dis* 67:159–173. <https://doi.org/10.1111/2049-632X.12033>.
- Boucher HW, Talbot GH, Bradley JS, Edwards JE, Gilbert D, Rice LB, Scheld M, Spellberg B, Bartlett J. 2009. Bad bugs, no drugs: no ESKAPE! An update from the Infectious Diseases Society of America. *Clin Infect Dis* 48:1–12. <https://doi.org/10.1086/595011>.
- Harmsen M, Yang L, Pamp SJ, Tolker-Nielsen T. 2010. An update on *Pseudomonas aeruginosa* biofilm formation, tolerance, and dispersal. *FEMS Immunol Med Microbiol* 59:253–268. <https://doi.org/10.1111/j.1574-695X.2010.00690.x>.
- Poole K. 2011. *Pseudomonas aeruginosa*: resistance to the max. *Front Microbiol* 2:65. <https://doi.org/10.3389/fmicb.2011.00065>.
- World Health Organization. 2017. Prioritization of pathogens to guide discovery, research and development of new antibiotics for drug-resistant bacterial infections, including tuberculosis. World Health Organization, Geneva, Switzerland.
- Fernebro J. 2011. Fighting bacterial infections—future treatment options. *Drug Resist Updat* 14:125–139. <https://doi.org/10.1016/j.drug.2011.02.001>.
- Bender KO, Garland M, Ferreyra JA, Hryckowian AJ, Child MA, Puri AW, Solow-Cordero DE, Higginbottom SK, Segal E, Banaei N, Shen A, Sonnenburg JL, Bogoyo M. 2015. A small-molecule antivirulence agent for treating *Clostridium difficile* infection. *Sci Transl Med* 7:306ra148. <https://doi.org/10.1126/scitranslmed.aac9103>.
- D'Angelo F, Baldelli V, Halliday N, Pantalone P, Polticelli F, Fiscarelli E, Williams P, Visca P, Leoni L, Rampioni G. 2018. Identification of FDA-approved drugs as antivirulence agents targeting the pqs quorum-sensing system of *Pseudomonas aeruginosa*. *Antimicrob Agents Chemother* 62:e01296-18. <https://doi.org/10.1128/AAC.01296-18>.
- Kong C, Neoh HM, Nathan S. 2016. Targeting *Staphylococcus aureus* toxins: a potential form of anti-virulence therapy. *Toxins (Basel)* 8:72. <https://doi.org/10.3390/toxins8030072>.
- Romo JA, Pierce CG, Chaturvedi AK, Lazzell AL, McHardy SF, Saville SP, Lopez-Ribot JL. 2017. Development of anti-virulence approaches for candidiasis via a novel series of small-molecule inhibitors of *Candida albicans* filamentation. *mBio* 8:e01991-17. <https://doi.org/10.1128/mBio.01991-17>.
- Smith KM, Bu Y, Suga H. 2003. Induction and inhibition of *Pseudomonas aeruginosa* quorum sensing by synthetic autoinducer analogs. *Chem Biol* 10:81–89. [https://doi.org/10.1016/s1074-5521\(03\)00002-4](https://doi.org/10.1016/s1074-5521(03)00002-4).
- Soukarieh F, Vico Oton E, Dubern JF, Gomes J, Halliday N, de Pilar Crespo M, Ramirez-Prada J, Insuasty B, Abonia R, Quiroga J, Heeb S, Williams P, Stocks MJ, Camara M. 2018. In silico and in vitro-guided identification of inhibitors of alkylquinolone-dependent quorum sensing in *Pseudomonas aeruginosa*. *Molecules* 23:257. <https://doi.org/10.3390/molecules23020257>.
- Maura D, Ballok AE, Rahme LG. 2016. Considerations and caveats in antivirulence drug development. *Curr Opin Microbiol* 33:41–46. <https://doi.org/10.1016/j.mib.2016.06.001>.
- Stover CK, Pham XQ, Erwin AL, Mizoguchi SD, Warren P, Hickey MJ, Brinkman FS, Hufnagle WO, Kowalik DJ, Lagrou M, Garber RL, Goltry L, Tolentino E, Westbrook-Wadman S, Yuan Y, Brody LL, Coulter SN, Folger KR, Kas A, Larbig K, Lim R, Smith K, Spencer D, Wong GK, Wu Z, Paulsen IT, Reizer J, Saier MH, Hancock RE, Lory S, Olson MV. 2000. Complete genome sequence of *Pseudomonas aeruginosa* PAO1, an opportunistic pathogen. *Nature* 406:959–964. <https://doi.org/10.1038/35023079>.
- Winsor GL, Griffiths EJ, Lo R, Dhillon BK, Shay JA, Brinkman FS. 2016. Enhanced annotations and features for comparing thousands of *Pseudomonas* genomes in the *Pseudomonas* genome database. *Nucleic Acids Res* 44:D646–D653. <https://doi.org/10.1093/nar/gkv1227>.
- Rahme LG, Stevens EJ, Wolfort SF, Shao J, Tompkins RG, Ausubel FM. 1995. Common virulence factors for bacterial pathogenicity in plants and animals. *Science* 268:1899–1902. <https://doi.org/10.1126/science.7604262>.
- Finlay BB. 1999. Bacterial disease in diverse hosts. *Cell* 96:315–318. [https://doi.org/10.1016/s0092-8674\(00\)80544-9](https://doi.org/10.1016/s0092-8674(00)80544-9).
- Tan MW, Mahajan-Miklos S, Ausubel FM. 1999. Killing of *Caenorhabditis elegans* by *Pseudomonas aeruginosa* used to model mammalian bacterial pathogenesis. *Proc Natl Acad Sci U S A* 96:715–720. <https://doi.org/10.1073/pnas.96.2.715>.
- Apidianakis Y, Rahme LG. 2009. *Drosophila melanogaster* as a model host for studying *Pseudomonas aeruginosa* infection. *Nat Protoc* 4:1285–1294. <https://doi.org/10.1038/nprot.2009.124>.
- Chieda Y, Iiyama K, Yasunaga-Aoki C, Lee JM, Kusakabe T, Shimizu S. 2005. Pathogenicity of *gacA* mutant of *Pseudomonas aeruginosa* PAO1 in the silkworm, *Bombyx mori*. *FEMS Microbiol Lett* 244:181–186. <https://doi.org/10.1016/j.femsle.2005.01.032>.
- Koch G, Nadal-Jimenez P, Cool RH, Quax WJ. 2014. Assessing *Pseudomonas* virulence with nonmammalian host: *Galleria mellonella*. *Methods Mol Biol* 1149:681–688. [https://doi.org/10.1007/978-1-4939-0473-0\\_52](https://doi.org/10.1007/978-1-4939-0473-0_52).
- Clatworthy AE, Lee JS, Leibman M, Kostun Z, Davidson AJ, Hung DT. 2009. *Pseudomonas aeruginosa* infection of zebrafish involves both host and pathogen determinants. *Infect Immun* 77:1293–1303. <https://doi.org/10.1128/IAI.01181-08>.
- Dubern JF, Cigana C, De Simone M, Lazenby J, Juhas M, Schwager S, Bianconi I, Doring G, Eberl L, Williams P, Bragonzi A, Camara M. 2015. Integrated whole-genome screening for *Pseudomonas aeruginosa* virulence genes using multiple disease models reveals that pathogenicity is host specific. *Environ Microbiol* 17:4379–4393. <https://doi.org/10.1111/1462-2920.12863>.
- Wu JY, Siegel LM, Kredich NM. 1991. High-level expression of *Escherichia coli* NADPH-sulfite reductase: requirement for a cloned *cysG* plasmid to overcome limiting siroheme cofactor. *J Bacteriol* 173:325–333. <https://doi.org/10.1128/jb.173.1.325-333.1991>.
- Schnell R, Sandalova T, Hellman U, Lindqvist Y, Schneider G. 2005. Siroheme- and [Fe4-S4]-dependent NirA from *Mycobacterium tuberculosis* is a sulfite reductase with a covalent Cys-Tyr bond in the active site. *J Biol Chem* 280:27319–27328. <https://doi.org/10.1074/jbc.M502560200>.
- Ramirez JM, Del Campo FF, Paneque A, Losada M. 1966. Ferredoxin-nitrite reductase from spinach. *Biochim Biophys Acta* 118:58–71. [https://doi.org/10.1016/s0926-6593\(66\)80144-3](https://doi.org/10.1016/s0926-6593(66)80144-3).



27. Frangipani E, Perez-Martinez I, Williams HD, Cherbuin G, Haas D. 2014. A novel cyanide-inducible gene cluster helps protect *Pseudomonas aeruginosa* from cyanide. *Environ Microbiol Rep* 6:28–34. <https://doi.org/10.1111/1758-2229.12105>.
28. Sparacino-Watkins C, Stolz JF, Basu P. 2014. Nitrate and periplasmic nitrate reductases. *Chem Soc Rev* 43:676–706. <https://doi.org/10.1039/c3cs60249d>.
29. Lee DG, Urbach JM, Wu G, Liberati NT, Feinbaum RL, Miyata S, Diggins LT, He J, Saucier M, Deziel E, Friedman L, Li L, Grills G, Montgomery K, Kuchlerapati R, Rahme LG, Ausubel FM. 2006. Genomic analysis reveals that *Pseudomonas aeruginosa* virulence is combinatorial. *Genome Biol* 7:R90. <https://doi.org/10.1186/gb-2006-7-10-r90>.
30. Freschi L, Bertelli C, Jeukens J, Moore MP, Kukavica-Ibrulj I, Emond-Rheault JG, Hamel J, Fothergill JL, Tucker NP, McClean S, Klockgether J, de Souza A, Brinkman FSL, Levesque RC, Winstanley C. 2018. Genomic characterisation of an international *Pseudomonas aeruginosa* reference panel indicates that the two major groups draw upon distinct mobile gene pools. *FEMS Microbiol Lett* <https://doi.org/10.1093/femsle/fny120>.
31. Rojo F. 2010. Carbon catabolite repression in *Pseudomonas*: optimizing metabolic versatility and interactions with the environment. *FEMS Microbiol Rev* 34:658–684. <https://doi.org/10.1111/j.1574-6976.2010.00218.x>.
32. Behrends V, Ryall B, Zlosnik JE, Speert DP, Bundy JG, Williams HD. 2013. Metabolic adaptations of *Pseudomonas aeruginosa* during cystic fibrosis chronic lung infections. *Environ Microbiol* 15:398–408. <https://doi.org/10.1111/j.1462-2920.2012.02840.x>.
33. Arai H. 2011. Regulation and function of versatile aerobic and anaerobic respiratory metabolism in *Pseudomonas aeruginosa*. *Front Microbiol* 2:103. <https://doi.org/10.3389/fmicb.2011.00103>.
34. Moreno-Vivian C, Cabello P, Martinez-Luque M, Blasco R, Castillo F. 1999. Prokaryotic nitrate reduction: molecular properties and functional distinction among bacterial nitrate reductases. *J Bacteriol* 181:6573–6584. <https://doi.org/10.1128/JB.181.21.6573-6584.1999>.
35. Van Alst NE, Picardo KF, Iglewski BH, Haidaris CG. 2007. Nitrate sensing and metabolism modulate motility, biofilm formation, and virulence in *Pseudomonas aeruginosa*. *Infect Immun* 75:3780–3790. <https://doi.org/10.1128/IAI.00201-07>.
36. Van Alst NE, Wellington M, Clark VL, Haidaris CG, Iglewski BH. 2009. Nitrite reductase NirS is required for type III secretion system expression and virulence in the human monocyte cell line THP-1 by *Pseudomonas aeruginosa*. *Infect Immun* 77:4446–4454. <https://doi.org/10.1128/IAI.00822-09>.
37. Romeo A, Sonnleitner E, Sorger-Domenigg T, Nakano M, Eisenhaber B, Blasi U. 2012. Transcriptional regulation of nitrate assimilation in *Pseudomonas aeruginosa* occurs via transcriptional antitermination within the nirBD-PA1779-cobA operon. *Microbiology (Reading)* 158:1543–1552. <https://doi.org/10.1099/mic.0.053850-0>.
38. Akhtar S, Khan A, Sohaskey CD, Jagannath C, Sarkar D. 2013. Nitrite reductase NirBD is induced and plays an important role during in vitro dormancy of *Mycobacterium tuberculosis*. *J Bacteriol* 195:4592–4599. <https://doi.org/10.1128/JB.00698-13>.
39. Nathan C, Shiloh MU. 2000. Reactive oxygen and nitrogen intermediates in the relationship between mammalian hosts and microbial pathogens. *Proc Natl Acad Sci U S A* 97:8841–8848. <https://doi.org/10.1073/pnas.97.16.8841>.
40. Sohaskey CD, Wayne LG. 2003. Role of narK2X and narGHJ in hypoxic up-regulation of nitrate reduction by *Mycobacterium tuberculosis*. *J Bacteriol* 185:7247–7256. <https://doi.org/10.1128/jb.185.24.7247-7256.2003>.
41. Pessi G, Haas D. 2000. Transcriptional control of the hydrogen cyanide biosynthetic genes hcnABC by the anaerobic regulator ANR and the quorum-sensing regulators LasR and RhIR in *Pseudomonas aeruginosa*. *J Bacteriol* 182:6940–6949. <https://doi.org/10.1128/jb.182.24.6940-6949.2000>.
42. Kirchner S, Fothergill JL, Wright EA, James CE, Mowat E, Winstanley C. 2012. Use of artificial sputum medium to test antibiotic efficacy against *Pseudomonas aeruginosa* in conditions more relevant to the cystic fibrosis lung. *J Vis Exp* 2012:e3857. <https://doi.org/10.3791/3857-e3857>.
43. Grasmann H, Ioannidis I, Tomkiewicz RP, de Groot H, Rubin BK, Ratjen F. 1998. Nitric oxide metabolites in cystic fibrosis lung disease. *Arch Dis Child* 78:49–53. <https://doi.org/10.1136/adc.78.1.49>.
44. Palmer KL, Aye LM, Whiteley M. 2007. Nutritional cues control *Pseudomonas aeruginosa* multicellular behavior in cystic fibrosis sputum. *J Bacteriol* 189:8079–8087. <https://doi.org/10.1128/JB.01138-07>.
45. Sambrook JF, Russell SA. 2001. *Molecular cloning: a laboratory manual*, 3rd ed. Cold Spring Harbor Laboratory Press, Cold Spring Harbor, NY.
46. Essar DW, Eberly L, Hadero A, Crawford IP. 1990. Identification and characterization of genes for a second anthranilate synthase in *Pseudomonas aeruginosa*: interchangeability of the two anthranilate synthases and evolutionary implications. *J Bacteriol* 172:884–900. <https://doi.org/10.1128/jb.172.2.884-900.1990>.
47. Lore NI, Cigana C, De Fino I, Riva C, Juhas M, Schwager S, Eberl L, Bragonzi A. 2012. Cystic fibrosis-niche adaptation of *Pseudomonas aeruginosa* reduces virulence in multiple infection hosts. *PLoS One* 7:e35648. <https://doi.org/10.1371/journal.pone.0035648>.
48. Pirone L, Bragonzi A, Farcomeni A, Paroni M, Auriche C, Conese M, Chiarini L, Dalmastrì C, Bevivino A, Ascenzioni F. 2008. *Burkholderia cenocepacia* strains isolated from cystic fibrosis patients are apparently more invasive and more virulent than rhizosphere strains. *Environ Microbiol* 10:2773–2784. <https://doi.org/10.1111/j.1462-2920.2008.01697.x>.
49. Ulrich M, Beer I, Braitmaier P, Dierkes M, Kummer F, Krismer B, Schumacher U, Grapler-Mainka U, Riethmüller J, Jensen PO, Bjarnsholt T, Hoiby N, Bellon G, Döring G. 2010. Relative contribution of *Prevotella intermedia* and *Pseudomonas aeruginosa* to lung pathology in airways of patients with cystic fibrosis. *Thorax* 65:978–984. <https://doi.org/10.1136/thx.2010.137745>.
50. Hoffmann N, Rasmussen TB, Jensen PO, Stub C, Hentzer M, Molin S, Ciofu O, Givskov M, Johansen HK, Hoiby N. 2005. Novel mouse model of chronic *Pseudomonas aeruginosa* lung infection mimicking cystic fibrosis. *Infect Immun* 73:2504–2514. <https://doi.org/10.1128/IAI.73.4.2504-2514.2005>.
51. Bragonzi A, Worlitzsch D, Pier GB, Timpert P, Ulrich M, Hentzer M, Andersen JB, Givskov M, Conese M, Döring G. 2005. Nonmucoid *Pseudomonas aeruginosa* expresses alginate in the lungs of patients with cystic fibrosis and in a mouse model. *J Infect Dis* 192:410–419. <https://doi.org/10.1086/431516>.